Published in final edited form as:
Electrophoresis. 2010 April ; 31(7): 1162–1174. doi:10.1002/elps.200900739.

Capillary electrochromatography-atmospheric pressure ionization mass spectrometry of pesticides using a surfactant-bound monolithic column

Congying Gu and **Shahab A. Shamsi***
Department of Chemistry, Center for Biotechnology and Drug Design, Georgia state University, Atlanta, GA 30303, USA.

Abstract

A surfactant bound poly (11-acrylaminoundecanoic acid-ethylene dimethacrylate) (AAUA-EDMA) monolithic column was simply prepared by in-situ co-polymerization of AAUA and EDMA with 1-propanol, 1,4-butanediol and water as porogens in 100 μm id fused silica capillary in one step. This column was used in capillary electrochromatography (CEC)-atmospheric pressure photoionization (APPI)-mass spectrometry system for separation and detection of *N*-methylcarbamates (NMCs) pesticides. Numerous parameters are optimized for CEC-APPI-MS. After evaluation of the mobile phase composition, sheath liquid composition and the monolithic capillary outlet position, a fractional factorial design (FFD) was selected as a screening procedure to identify factors of ionization source parameters, such as sheath liquid flow rate, drying gas flow rate, drying gas temperature, nebulizing gas pressure, vaporizer temperature, and capillary voltage, which significantly influence APPI-MS sensitivity. A face-centered central composite design (CCD) was further utilized to optimize the most significant parameters and predict the best sensitivity. Under optimized conditions signal-to-noise ratios (*S/N*) around 78 were achieved for an injection of 100 ng/mL of each pesticide. Finally, this CEC-APPI-MS method was successfully applied to the analysis of nine NMCs in spiked apple juice sample after solid phase extraction with recoveries in the range of 65 to 109%.

Keywords

11-Acrylaminoundecanoic acid (AAUA) monomer; Atmospheric pressure photoionization APPI; Experimental design; Monolith; *N*-methyl carbamates (NMCs) pesticides

1 Introduction

The combination of capillary zone electrophoresis (CZE) with mass spectrometry (MS) is now considered a well-established multidimensional approach. On one side CZE is very attractive for providing high efficiency separation of charged compounds, while on the other side MS provide not only molecular mass but also structural information [1–2]. However, CZE-MS using volatile buffers (e.g., ammonium carbonate, trifluoroacetic acid) often may result in less than optimal peak shapes, lower separation selectivity for charged compounds and no separation of neutral compounds from one another. One would expect the performance of CE-MS to increase with the use of a pseudostationary phase (e.g., the use of micelles in MEKC-MS) or a fixed stationary phase (e.g., packed column in CEC-MS).

***Corresponding author:** Professor Shahab A. Shamsi, Department of Chemistry, Center for Biotechnology and Drug Design, Georgia state University, Atlanta, GA 30303, USA. Phone: 404-413-5512; Fax: 404-413-5505; chesas@langate.gsu.edu.

Unfortunately, the use of conventional micelles in MEKC-MS causes unavoidable signal suppression. Partial-filling approach, which incorporates a plug of micelles in the running buffer has been successfully implemented, but the resolution of closely eluting compounds is seriously compromised. In addition, the plug length of the micelles must be carefully optimized. On the other hand, the use of packed columns in CEC-MS with two sintered frits (one at the inlet and the other at the outlet end) to retain the stationary phase offers obvious option to MEKC-MS. However, it has also suffered from several drawbacks, such as lack of reproducibility of sintered frits as well as poor permeability and fragility. Perhaps, the most serious drawback for packed column CEC-MS is the bubble formation when the outlet end is exposed to the high-temperature of the spray chamber [3].

To solve these aforementioned problems associated with MEKC-MS and CEC-MS two valuable approaches such as the use of molecular micelles for MEKC-MS [4–5], and the use of internally tapered single-frit columns [6–7] for CEC-MS have been developed as possible alternatives for high efficient separation and highly sensitive detection of various classes of achiral and chiral molecules [8–11]. Surfactant-bound monolithic column, which is usually prepared by in-situ polymerization of surfactant monomers immobilized on a capillary column, is an attractive alternative to packed column CEC-MS because the column requires no frit to hold stationary phases. Moreover, the surfactant-bound CEC-MS columns simply avoid the use of surfactant forming micelles in the running buffer. Other advantages of surfactant-bound monoliths [12–13], which are similar to other types of monolithic columns used in CEC include fine-tuned pore structure, easy column preparation procedure, no need of frit, which will decrease the risk of bubble formation as well as providing improve reproducibility and ruggedness for CE-MS [14–16].

Among the available ionization sources, electrospray ionization (ESI) have dominated its use in CZE, MEKC and CEC, while there have been some examples of atmospheric pressure chemical ionization (APCI) for CE-MS [7,17]. The ESI and APCI ionizaton methods are based on the charge affinity of analyte molecule in the gas phase. Atmospheric pressure photoionization (APPI) is a relatively new ionization source, which works on a photoionization of the analyte interacting with photons emitted by a krypton discharge lamp at 10.03 and 10.6 eV in 4:1 ratio, which is higher than most of the ionization energy (IE) of analytes (7~10 eV), but lower than those of the atmospheric gases and the mobile phase. Thus, photoionization allows ions from the analytes to be selectively produced without ionizing the mobile phase thereby reducing ion suppression effects [18–19]. Analytes that are not directly or weakly ionized by photons can be ionized via a proton transfer or charge transfer mechanism using a dopant (*e.g.*, acetone or toluene). There are ranges of compounds, which cannot be efficiently ionized by ESI or APCI. Under such conditions APPI has become the source of choice for many CE applications [20–23]. Moreover, it has been shown that APPI is somewhat unaffected by the nonvolatile CE buffers, such as sodium or potassium salts with phosphate and borate anions [24]. It is well-known that the use of non-volatile buffers may contaminate the ESI ionization chamber and cause ion suppression. On the other hand, APPI is compatible with these non-volatile buffers. Although several attractive applications have been explored using LC-APPI-MS [20,25–27], there have been only few reports on the combination of packed [28] or sol-gel [29] CEC columns with APPI-MS, but none on the use of monolithic columns for APPI-MS.

N-methyl carbamates (NMCs) pesticides, due to their relatively low mammalian oral and dermal toxicity are widely used in homes, gardens and agriculture. However, researches have shown that accumulation of carbamate residues in food chain could affect the nervous system by reducing the ability of cholinesterase, an enzyme used in regulating the neurotransmitter acetylcholine [30–31]. Hence, recent concerns have stimulated increasing awareness and testing of these compounds in complicated food and environmental matrices

[32–34]. A recent paper pointed out the sensitivity advantages of LC-APPI-MS over LC-APCI-MS for the determination of several pesticides [35], but no work is reported so far on their analysis by CEC-APPI-MS.

The purpose of this work is to introduce APPI as a new ionization method for CEC-MS using an approach based on surfactant-bound monolithic column. Next, the suitability and compatibility of this new hyphenation technology was tested for the determination of NMC pesticides. To the best of our knowledge, the combination of APPI-MS with monolithic column in CEC has never been investigated. First, CEC columns based on 11-acrylaminoundecanoic acid-ethylene dimethyacrylate (AAUA-EDMA) monolithic column was prepared to achieve baseline separation of the nine NMCs. Second, the fragmentor voltage, capillary outlet position and sheath liquid composition was optimized using a univariate approach. Because of potential interactions between spray chamber parameters, a multivariate optimization involving fractional factorial design (FFD) was conducted to screen the most important chamber parameters that affect the APPI-MS sensitivity. A central composite design (CCD) was next used to fine tune and optimize the most important parameters to achieve the best signal-to-noise (*S/N*) ratio for the NMCs. Finally, the potential application of this optimized method was applied to the determination of NMC pesticides in fruit juices at low concentrations.

2 Materials and methods

2.1 Reagents and materials

The crosslinker, ethylene dimethacrylate (EDMA), the porogen 1-propanol, the initiator 2, 2′-azobisisobutyronitrile (AIBN), and the monomer 11-aminoundecanoic acid were all purchased from Aldrich (Milwaukee, WI, USA). Compounds such as γ-methacryloxypropyltrimethoxy-silane, acryloyl chloride, acetonitrile (ACN), 1M ammonium acetate (NH_4OAC) solution and all *N*-methyl-carbamates (NMCs) were obtained from Sigma (St. Louis, MO, USA). The other porogen 1,4-butanediol and the other monomer butyl methacrylate were purchased from Fluka (Buchs, Switzerland). All the reagents were used as received except for the EDMA, which was purified by distillation under vacuum prior to use. Fused silica capillaries (100 μm ID 00D7 365 μm OD) were obtained from Polymicro Technologies Inc (Phoenix, AZ, USA).

2.2 Preparation of AAUA monomer

First, an aqueous solution of ethanol (250 mL ethanol /35 mL triply distilled water) was used to dissolve 10 g of 11-aminoundecanoic acid. To this solution, 6 g of NaOH was added slowly until a clear solution is obtained. Next, 6 mL of acryloyl chloride was added dropwise and the reaction mixture stirred for approximately three hours at just below 10 °C, after which it was filtered. The filtrate was acidified with diluted hydrochloric acid and washed with triply deionized water. The white precipitate formed was collected after filtration. The crude product was recrystallized from aqueous ethanol, filtered and dried by lyophilization [36–37]. The purity of AAUA was checked by electrospray ionization mass spectrometry (ESI-MS), ^1H NMR and elemental analysis.

2.3 Preparation of AAUA-EDMA monolith

The preparation of AAUA monolith has been thoroughly studied in our previous work [12,13]. Briefly, for the preparation of stationary phases the inner walls of the fused silica capillaries were first vinylized with 3-(trimethoxylsilyl)propyl methacrylate. The procedure can be found else-where [38–39]. Subsequently, 7% (w/w) AAUA, 18.5% (w/w) EDMA, 60% (w/w) 1-propanol, 2% (w/w) 1,4-butanediol, (12%) water, and 0.5% (w/w) AIBN were mixed ultrasonically into a homogenous solution and purged with nitrogen for 10 min. A 65

cm long silanized capillary was filled with the polymerization mixture up to a length of 42 cm, sealed with rubber septum, and then placed in a GC oven to polymerize for 20 h at 60 °C. The ternary porogenic system including 1, 4-butanediol, 1-propanol and water were borrowed from previous work [40]. After the polymerization was completed, the monolithic column was washed with ACN using a HPLC pump to remove unreacted monomers and porogens. Finally, the column was cut to 60 cm with an effective length of 40 cm.

2.4 CEC-APPI-MS instrumentation, parameters, and conditions

All CEC-MS experiments were carried out with an Agilent 3D capillary electrophoresis instrument interfaced to a single quadrupole mass spectrometer (Agilent Technologies, Palo Alto, CA). An Agilent 1100 series HPLC pump equipped with 1:100 splitter was used to deliver the sheath liquid. The Agilent Chemstation software (Version 10.02) was used for instrumental control and data processing. The APPI source was equipped with a spacer and krypton discharge lamp emitting photons (*hv* = 10.01 eV) also supplied by Agilent Technologies.

APPI-MS of NMCs was performed in selected-ion monitoring mode as group SIM. For oxamyl, ammonium adduct ions $[M+NH_4\text{-}CH_3NHCOO]^+$ was the most abundant, hence selected as target ion. For aldicarb, $[M+H\text{-}(CH_3NHCOOH)]^+$ was the target ion. For other NMCs, highest intensity protonated molecular ions $[M + H]^+$ were selected as the target ions. The details of NMC target ions are listed in Table 1.

The CEC-MS running mobile phase was different concentration of ACN in 5 mM NH_4OAC at pH 6.5. A constant voltage of 30 kV was applied during analysis. Samples were kept at 20 °C in the autosampler and injected at 5kV for 3s.

2.5 Preparation of standard analytes

Individual stock solutions (A) of the NMCs pesticides were prepared at a concentration of 1mg/mL in pure ACN. The working standard solution (B) containing 10 μg/mL of all the NMCs was prepared in ACN. For method development, a solution containing a mixture of each NMC at 100 ng/mL was used. To prepare a calibration curve, the working standard solution was diluted to the final working concentrations of 5, 10, 25, 50, 100, 200 and 500 ng/mL in ACN. The structures of the NMCs (along with log *P* and *pKa* values) are shown in Figure 1.

2.6 Sample preparation

Apple juice sample was collected from a local grocery store. For the preparation of fortified samples, 10 μL of the 10 μg/mL standard working solution B was added to the 10 mL of juice sample. Before extraction, the Oasis HLB column (Waters, Milford, MA, USA, 3 cm^3, 60mg) was conditioned with 3 mL of tertbutylmethyl ether, followed by 3 mL of HPLC grade methanol and finally 3 mL of triply deionized water by applying a slight vacuum. The juice sample was passed through the HLB column and then eluted with three aliquots of 3 mL of methanol/-tertbutylmethyl ether [10:90,(v/v)]. The eluate was evaporated to dryness under nitrogen at 40 °C. Finally, the extract was reconstituted with 2 mL of methanol/ dichloromethane (1:99, v/v).

The next step requiring clean-up of other unwanted components [41]. First, the aminopropyl column (Waters, Milford, MA, USA, 6 cm^3, 500mg) was conditioned with 4 mL of methanol/dichloromethane (1:99, v/v). Sample extract was then added to the aminopropyl column and eluted dropwise with 2.0 mL of methanol-dichloromethane (1:99, v/v) from the cartridge under a slight vacuum. Such elution procedure was repeated twice with another 1.0 mL of methanol/dichloromethane (1:99, v/v). All of the three effluents were collected and

then evaporated to dryness under nitrogen at 40 °C. The final dry extract was reconstituted in 1.0 mL of ACN/water (35:65, v/v), and filtered with 0.22 μm membrane filter before analysis.

2.7 Calculation of relative sensitivity and capacity factor

The relative sensitivity ($(S/N)_{\%,i}$) of an analytes under condition *i* was calculated according to equation (1),

$$\left(S/N\right)_{\%,i} = \frac{\left(S/N\right)_i}{\left(S/N\right)_{\max}} \times 100\% \quad (1)$$

where, $(S/N)_i$ is the signal to noise ratio of an analyte under one specific condition *i*, $(S/N)_{max}$ is the highest *S/N* of the same analyte under any specific conditions.

The k-values was determined by the following equation: $k = \frac{t - t_0}{t_0}$. The t_0 was determined using thiourea as an unretained compound.

2.8 Experimental design software

Design-Expert (version 7.0.3, Stat-Ease, Inc. Minneapolis, MN) was used to generate the fractional factorial design (FFD), central composite design (CCD), data processing (statistical calculations) and response surface data analysis to predict optimum conditions. The detail information about the working principle of the software could be found in our previous publications [12,42].

3 Results and discussion

3.1 Optimization of mobile phase composition

Various composition of 5 mM NH_4OAC buffers in combination with methanol or ACN were evaluated as possible mobile phases. As discussed in the literature, methanol is preferred eluent over ACN for LC-APPI-MS due to improved sensitivity [20,35]. However, it should be noted that the effluent of the CEC column is substantially diluted with sheath liquid, and the solvent present in the latter will dominate ionization efficiency. Thus, the use of methanol in mobile phase has no significant sensitivity advantage over ACN. In fact, when methanol was replaced with ACN significantly shorter retention times with improved chromatographic resolutions of NMCs were observed. Therefore, various volume fraction of ACN from 25% to 40% were used to optimize the chromatographic separation of nine NMCs. The electrochromatograms shown in Supporting Information (Figure 1) demonstrate that with the increase of %ACN, retention times of the NMCs get shorter while resolutions get worse. For example, resolution between peak 3 and peak 4 changed from 2.7 to 0.4 when %ACN increasing from 25% to 40%, while t_R of the last eluting peak decreased from 17.6 to 10.7 min. Thus, a 35% ACN in the mobile phase was finally selected as the best compromise between resolution and analysis time.

Figure 2 shows plots of log *k´* as a function of %ACN. The retention mechanism of hydrophobic NMCs (i.e., aldicarb-methiocarb, log *P* = 1.13 to 2.89) seems to follow reversed-phase chromatography behavior as confirmed by the linear relationship of log *k´ versus* % ACN. However, for the least retained and hydrophilic solutes (i.e., oxamyl, methomyl, log *P* = −0.47 to 0.60), the plots deviate from linearity indicating the occurrence

of both hydrophilic and hydrophobic interactions with the AAUA-EDMA stationary phase. When two distinct interaction processes (*i.e.* hydrophobic and hydrophilic interaction) contribute to solute retention, the retention factor k' is given by:

$$k' = x_i k_i + x_j k_j \quad (2)$$

where x_i and x_j are the hydrophobic and hydrophilic phase ratios, respectively, and k_i and k_j are their corresponding distribution coefficients. This means the k' values for each retention process are additive [43–44]. Equation (2) may explain the retention trend observed in Figure 2. At higher water content, reversed-phase or hydrophobic interaction predominate for all NMCs retention, whereas at higher %ACN the hydrophilic interaction predominate (resulting in longer retention of oxamyl and to some extent methamoyl). On the other hand, at intermediate %ACN, both interactions contribute to the NMCs retention depending on their relative polar character.

3.2 Optimization of capillary outlet position

Several previous works on open tubular capillary stated that capillary outlet position will affect the ionization efficiency and consequently the APPI-MS sensitivity [24,45–46]. Experiments with the monolithic capillary positioned from 0 mm to (±) 0.6 mm inside and outside the needle were conducted. Experimental results (shown in Supporting Information,Figure 2) indicated that the displacement of capillary outside the needle (e.g., +0.2 mm and +0.4 mm) provided lower intensity due to perturbation of the Taylor cone. However, further increase in protruding length of capillary at +0.6 mm promotes a suction effect increasing the intensity. On the other hand, when capillary is positioned at −0.4 mm or −0.6 mm inside the needle it provided overall better sensitivity (due to increasing ionization) for most of the NMCs.

3.3 Optimization of fragmentor voltage

The fragmentor voltage is applied to the exit of the glass capillary (located inside the ionization source of the spray chamber) and affects the transmission and fragmentation of sample ions between the exit of the glass capillary and the skimmer at relatively high pressure ~ 3 Torr (1 Torr = 5133.322 Pa) [47]. To determine the optimal fragmentor voltage, the intensities of these ions were compared at the fragmentor voltages of 56, 60, 65, 70, 80 and 100 V (shown in Supporting Information, Figure 3). Overall 60 V was chosen as a best compromise for all nine carbamates as optimized fragmentor voltage.

3.4 Optimization of sheath liquid composition

Sheath liquid, usually consisting of organic solvent, electrolyte and photoionizable molecules (e.g., toluene, acetone), which could ground the CEC voltage and provide proper conditions for ionization. Therefore, it plays an important role in ionization efficiency and sensitivity of CEC-APPI-MS system. Various concentrations of NH_4OAC, acetone and methanol in the sheath liquid were optimized, respectively.

Figure 3A demonstrate the effect of the concentration of NH_4OAC on the relative sensitivity. The use of 5 mM NH_4OAC in the sheath liquid provided the best overall sensitivity for all the pesticides. A suitable substance, added in relatively large amounts to the sheath liquid, could significantly increase the number of ions through photoionization. Such a substance is called a dopant [48]. Photoionization initiates the formation of dopant radical cations that react through proton transfer or charge exchange with analytes having lower ionization energies (IEs). Acetone and toluene are two most often used dopants in APPI, the mechanism is believed to be either proton-transfer or charge-exchange reactions.

Because the choice of dopant is an important factor affecting the sensitivity under APPI we tested acetone and toluene, which are previously reported as two useful dopants [35]. However, only acetone gave significant enhancement in sensitivity of NMCs. Figure 3B illustrates the effect of the concentration of acetone (v/v) on the sensitivity. It is clear that increasing the volume fraction of acetone from 0% to 2% in the sheath liquid, increases the relative intensity of the target ions. However, at higher than 2%, the average intensity of the target ions drops. Based on the above results, 2% acetone was chosen as the optimized volume fraction of dopant. Figure 3C shows the effect of the composition of sheath liquid, methanol on the sensitivity. At 25% (v/v) of MeOH, sensitivity was only slightly lower compare to 50% (v/v) of MeOH. However, a significant decrease in relative sensitivity was observed at higher proportion [i.e., 75% (v/v)] of MeOH. Hence, at a volume fraction of 50% (v/v) MeOH, the optimum sensitivity was achieved for eight out of the nine pesticides.

3.5 Optimization of ionization source conditions by experimental design

3.5.1 Screening of the most important parameters—The spray chamber parameters such as drying gas temperature (DGT), drying gas flow rate (DGF), nebulizer pressure (NP), capillary voltage (CV), sheath liquid flow rate (SLF) and vaporizer temperature (VT) are very important parameters for APPI sensitivity. To optimize the aforementioned parameters, a FFD experimental design was used to find the most important parameters for further optimization.

The upper and lower values of the levels for the spray chamber parameters were set according to preliminary experiments and the limits of the APPI instrument. The investigated ranges of the factors are listed in Table 2. As shown in Table 3, twenty-two random runs using a half FFD were performed to estimate the experimental error. Average sensitivity ($S/N_{(avg)}$) and average peak area ($Peak\ area_{(avg)}$) were set as analytical responses. Under the investigated range, the $S/N_{(avg)}$ ranged from 24 to 99, while $Peak\ area_{(avg)}$ ranged from 1.9×10^5 to 1.0×10^6. This indicated that the chamber parameters of the APPI source have significant effects on the sensitivity of the NMCs and these parameters should be carefully optimized.

A linear regression model was developed for each response. The yielded model is a mathematical equation, which is useful for identifying the relative significance of the factors by directly comparing the factor coefficients. Positive interaction coefficients indicate the corresponding factor is directly proportional to the response and *vise versa*. Figure 4A and 4B demonstrates the regression coefficient plots for the responses, $S/N_{(avg)}$ and $Peak\ area_{(avg)}$, respectively. The 95% confidence interval was expressed in terms of error bar over the coefficient. If the coefficient is smaller than the interval, the variation of the response caused by changing the variable is smaller than the experimental error. Under such situation, the variable is considered not to be significant. For example, as shown in Figure 4A, NP, CV and VT were found to have no significant effect on the sensitivity. In addition, note that DGF and DGT play negative effects on $S/N_{(avg)}$, whereas SLF plays a positive effect on the $S/N_{(avg)}$. For the $Peak\ area_{(avg)}$ (Figure 4B), DGF and SLF were the two most significant parameters with DGF showing a negative effect, whereas SLF shows a positive effect.

The validation of the calculated empirical model was conducted by ANOVA. The ANOVA data (including sum of squares, mean square, F-value and Prob>F values, R^2, Adj-R^2, Pred-R^2, Adeq-R^2) for the model are listed in Table 4. At first, the model F-value and Prob >F value were checked. The F-value, which was calculated by dividing model mean square with residual mean square, is tested for comparing model variance with residual variance. If the ratio is close to one, then this is unlikely that any of the factors have a significant effect on the response. As shown in Table 4 (second and seventh rows), the model F-values for *S/*

$N_{(avg)}$ and *Peak area*$_{(avg)}$ are 11 and 16, respectively, which indicate that both models are significant. The Prob >F value indicates the probability of seeing the observed F-value if the null hypothesis is true. In general, a term that has a Prob >F value less than 0.05 would be considered a significant effect, while a Prob >F value greater than 0.10 is generally regarded as not significant. The model Prob>F vales for $S/N_{(avg)}$ and *Peak area*$_{(avg)}$ are 0.0001 and <0.0001, respectively, which means that there is at least one significant factors for each model. The lack of fit F-values and Prob> F values listed in fourth and ninth rows in Table 4 indicate that the "Lack of fit" of all the models are not significant, The R^2 (multiple correlation coefficient), Adj-R^2, Pred-R^2 and adequate precision values (Ade-pre) for the models are shown in eighth to eleventh columns in Table 4. For a good statistical model, R^2 value should be close to 1.0 and difference between adj-R^2 and pred-R^2 should be within 0.2. For all the models, the three values are all within acceptable range. The Ade-pre value is an index of the signal to noise ratio and a value bigger than 4 suggests that the model gives a good fit [49]. The Ade-pre of the models are 11.2 and 13.8 for the responses ($S/N_{(avg)}$ and *Peak area*$_{(avg)}$) suggesting that the models could be used to navigate the design space.

3.5.2 Further optimization using central composite design—From the results of FFD, it is found that DGF, SLF and DGT are the three most important factors for $S/N_{(avg)}$ and *Peak area*$_{(avg)}$. A central composite design (CCD) was used to further optimize these three ionization source parameters. Variables and their ranges are summarized in Table 5 and the limits of the ranges were defined based on the preliminary FFD experiments. Briefly, 20 experiments were carried out in total including 6 central points, which could provide repeatability information. Table 6 demonstrates the detailed design and responses for all runs generated by the CCD. The $S/N_{(avg)}$ and *Peak area*$_{(avg)}$ for the nine NMCs pesticides were set as responses. The error of the repetitive runs was compared with the excess design points by *F*-test to determine the significance of the critical factors. As shown in Table 6, the $S/N_{(avg)}$ ranged from 30 to 91, whereas the *Peak area*$_{(avg)}$ ranged from 2.7×10^5 to 1.1×10^6. The RSD values for the repeatability of $S/N_{(avg)}$ and *Peak area*$_{(avg)}$ of the six central points, were 5.8% and 8.6%, respectively, which indicated that the experimental error were low. Table 7 shows the statistical parameters of the CCD design. The rules to judge this parameter (discussed in section 3.5.1) suggest that all the statistic values are within the acceptable ranges.

Response surface plots provide clear view of the trend. Figure 5A–C presents the response surface plot for $S/N_{(avg)}$. Figure 5A, reveals that decreasing the DGF and increasing the SLF, there is an increasing trend for $S/N_{(avg)}$. However, decreasing both the DGF and DGT an increased $S/N_{(avg)}$ could be achieved (Figure 5B). From Figure 5C, it is clear that decreasing DGT and increasing SLF, there is an increasing trend for $S/N_{(avg)}$. Similar trends were found for *Peak area*$_{(avg)}$ (data not shown).

In order to get a high sensitivity and high peak area simultaneously, Design-Expert uses Derringer's desirability function D(X) to obtain the best combination of the three factors (i.e., SLF, DGF and DGT). This function calculates the geometric mean of all transformed responses in the form of Equation (3):

$$D=(d_1 \times d_2 \times \cdots\cdots \times d_n)^{\frac{1}{n}}=\left(\prod_{i=1}^{n} d_i\right)^{\frac{1}{n}} \quad (3)$$

where d_i is the response (in our case, $S/N_{(avg)}$ and *Peak area*$_{(avg)}$) to be optimized, n is the number (in our case, two) of the response in the experimental design. *D* is the desirability that ranges from 0 (the least desirable) to 1 (the most desirable).

Using the aforementioned desirability function, the optimization parameters were obtained as follows: DGF 2 L/min, SLF 20 μL/min and DGT 200 °C. Under these optimized conditions, values of the responses (i.e. $S/N_{(avg)}$ and $Peak\ area_{(avg)}$) could also be predicted by the models. In order to evaluate the feasibility of this experimental design approach, the differences between the predicted values (obtained from the desirability function) and the experimental values (obtained from the real experimental) under the optimized condition were compared and the results are shown in Table 8. The experimental values for $S/N_{(avg)}$ and $Peak\ area_{(avg)}$ were 11% and 8% different from their predicted values, respectively. These differences are both within the normal ranges suggesting this experiment design is successful.

3.6 Sensitivity, linearity and precision

The performance of the CEC-APPI-MS method was evaluated by injecting a standard mixture of nine NMCs in group SIM. The calibration curves, regression coefficients (r^2), limit of detection (LOD, signal-to-noise=3) are all summarized in Table 9. The calibration curves for all pesticides showed good linearity (r^2>0.998) from 50 to 500 ng/mL. The LODs ranged from 3–30 ng/mL. We hypothesized that the differences in LODs for different NMCs is due to their differences in their ionization efficiency. The repeatability of the method was investigated by repetitive 5 injections at 100 ng/mL on one day and the relative standard deviation (RSD) of LODs ranged from 4.8% to 8.9%.

3.7 Analysis of apple juice

To demonstrate the suitability of CEC-APPI-MS, the method was successfully applied for the determination of NMCs pesticides in real samples such as apple juice sample. Figure 6 shows the electrochromatograms for the separation of blank apple juice and NCMs-spiked apple juice. It is clear that there are no NMCs detected in the blank apple juice. For the spiked apple juice, there are no additional interfering peaks. The recoveries for NMCs were calculated using spiked NMCs free apple juice. The average recoveries for each NCMs were in the range of 65 to 109% (inset table in Figure 6). Compared with previous work via LC-APPI-MS [41], obtained recoveries are in the similar range.

4 Concluding remarks

A CEC-APPI-MS method using a surfactant-bound AAUA-EDMA monolithic column is developed for the analysis of NMC pesticides. First, mobile phase composition, capillary outlet position, fragmentor voltage and sheath liquid composition were optimized. Second, a FFD was employed for screening the important factors of APPI-MS. The results showed that DGT, DGF and SLF are the three most important factors that affect the APPI-MS sensitivity. Next, the three important factors were fine tuned using a CCD design. To get the maximum sensitivity, the optimum combination of the three most important factors was predicted using Derringer's desirability function available in Design-Expert software. Differences of 8% and 11% between the predicted and the experimental values in terms of $S/N_{(avg)}$ and $Peak\ area_{(avg)}$ respectively, confirmed that the proposed approach is practical. Under the final optimized conditions, all 9 NMC pesticides were separated under 35 minutes and detected with a $S/N_{(avg)}$ around 78 (for an injection of 100 ng/mL of each compound). With an electrokinetic injection at 5 kV for 3s, the LOD for NMCs were in the range of 3–30 ng/mL. The apple juice sample spiked at a concentration of 10 ng/mL was used to demonstrate the feasibility of CEC-APPI-MS analysis for analysis of NMC pesticides. The recovery and repeatability of analysis were good enough for routine use.

Supplementary Material

Refer to Web version on PubMed Central for supplementary material.

Abbreviations

AAUA	11-acrylaminoundecanoic acid
APPI	atmospheric pressure photoionization
EDMA	ethylene dimethacrylate
NMCs	*N*-methyl carbamates

Acknowledgments

This work was supported by grant from the National Institutes of Health (Grant No. 2RO1-062314),American Chemical Society Petroleum Research Fund (PRF-47774-AC7)and Georgia State University, Scholarly Support Grant.

References

1. Schmitt-Kopplin P, Frommberger M. Electrophoresis. 2003; 24:3837–3867. [PubMed: 14661221]
2. Schmitt-Kopplin P, Frommberger M. Electrophoresis. 2005; 26:1209–1220. [PubMed: 15776480]
3. Klampfl CW. J. Chromatogr. A. 2004; 1044:131–144. [PubMed: 15354433]
4. Shamsi SA. Anal. Chem. 2001; 73:5103–5108. [PubMed: 11721906]
5. Akbay C, Rizvi SAA, Shamsi SA. Anal. Chem. 2005; 77:1672–1683. [PubMed: 15762571]
6. Zheng J, Norton D, Shamsi SA. Anal. Chem. 2006; 78:1323–1330. [PubMed: 16478129]
7. Norton D, Zheng J, Danielson ND, Shamsi SA. Anal. Chem. 2005; 77:6874–6886. [PubMed: 16255585]
8. Norton D, Shamsi SA. Anal. Chem. 2007; 79:9459–9470. [PubMed: 18001007]
9. Hou J, Zheng J, Shamsi SA. Electrophoresis. 2007; 28:1426–1434. [PubMed: 17465418]
10. Hou J, Zheng J, Shamsi SA. J. Chromatogr. A. 2007; 1159:208–216. [PubMed: 17499757]
11. Norton D, Rizvi SAA, Shamsi SA. Electrophoresis. 2006; 27:4273–4287. [PubMed: 17075924]
12. Gu C, He J, Jia J, Fang N, Shamsi SA. Electrophoresis. 2009; 30:3814–3827. [PubMed: 19885887]
13. Gu C, He J, Jia J, Fang N, Simmon R, Shamsi SA. J. Chromatogr. A. In Press.
14. Klodzinska E, Moravcova D, Jandera P, Buszewski B. J. Chromatogr. A. 2006; 1109:51–59. [PubMed: 16413561]
15. Svec F, Peters EC, Sýkora D, Yu C, Fréchet JMJ. J. High Res. Chromatogr. 2000; 23:3–18.
16. Zhu GJ, Zhang LH, Yuan HM, Liang Z, Zhang WB, Zhang YK. J. Sep. Sci. 2007; 30:792–803. [PubMed: 17536723]
17. Meyring M, Strickmann D, Chankvetadze B, Blaschke G, Desiderio C, Fanali S. J. Chromatogr. B. 1999; 723:255–264.
18. Lien GW, Chen CY, Wang GS. J. Chromatogr. A. 2009; 1216:956–966. [PubMed: 19118834]
19. Hommerson P, Khan AM, de Jong GJ, Somsen GW. Electrophoresis. 2007; 28:1444–1453. [PubMed: 17351894]
20. Robb DB, Covey TR, Bruins AP. Anal. Chem. 2000; 72:3653–3659. [PubMed: 10952556]
21. Hanold KA, Fischer SM, Cormia PH, Miller CE, Syage JA. Anal. Chem. 2004; 76:2842–2851. [PubMed: 15144196]
22. Cai SS, Syage JA, Hanold KA, Balogh MP. Anal. Chem. 2009; 81:2123–2128. [PubMed: 19227980]
23. Marchi I, Rudaz S, Veuthey JL. Talanta. 2009; 78:1–18. [PubMed: 19174196]
24. Nilsson SL, Andersson C, Sjöberg PJR, Bylund D, Petersson P, Jörntén-Karlsson M, Markides KE. Rapid Commun. Mass Sp. 2003; 17:2267–2272.

25. Bacaloni A, Callipo L, Corradini E, Giansanti P, Gubbiotti R, Samperi R, Lagana A. J. Chromatogr. A. 2009; 1216:6400–6409. [PubMed: 19656519]
26. Marchi I, Schappler J, Veuthey JL, Rudaz S. J. Chromatogr. B. 2009; 877:2275–2283.
27. Viglino L, Aboulfadl K, Prevost M, Sauve S. Talanta. 2008; 76:1088–1096. [PubMed: 18761160]
28. Zheng J, Shamsi SA. Anal. Chem. 2006; 78:6921–6927. [PubMed: 17007515]
29. Zheng J, Rizvi SAA, Shamsi SA, Hou J. J. Liq. Chromatogr. R. T. 2007; 30:43–57.
30. Bosgra S, van Eijkeren JCH, van der Schans MJ, Langenberg JP, Slob W. Toxicol. Appl. Pharm. 2009; 236:1–8.
31. Lowit, AB.; Ramesh, CG. Toxicology of Organophosphate & Carbamate Compounds. Burlington: Academic Press; 2006. p. 617-632.
32. Basheer C, Alnedhary AA, Rao BSM, Lee HK. J. Chromatogr. A. 2009; 1216:211–216. [PubMed: 19062025]
33. Ito Y, Goto T, Yamada S, Ohno T, Matsumoto H, Oka H, Ito Y. J. Chromatogr. A. 2008; 1187:53–57. [PubMed: 18295222]
34. Tadeo JL, Sánchez-Brunete C, Pérez RA, Fernández MD. J. Chromatogr. A. 2000; 882:175–191. [PubMed: 10895942]
35. Takino M, Yamaguchi K, Nakahara T. J. Agric. Food Chem. 2004; 52:727–735. [PubMed: 14969523]
36. Fujimoto C, Fujise Y, Kawaguchi S. J. Chromatogr. A. 2000; 871:415–425. [PubMed: 10735322]
37. Yeoh KW, Chew CH, Can LM, Koh LL, Teo HH. J. Macromol. Sci., Part A. 1989; 26:663–680.
38. Gu C, Lin L, Chen X, Jia J, Ren J, Fang N. J. Sep. Sci. 2007; 30:1005–1012. [PubMed: 17566334]
39. Gu C, Lin L, Chen X, Jia J, Ren J, Fang N. J. Chromatogr., A. 2007; 1170:15–22. [PubMed: 17915238]
40. Peters EC, Petro M, Svec F, Frechet JMJ. Anal. Chem. 1998; 70:2288–2295. [PubMed: 9624900]
41. Rawn DFK, Roscoe V, Krakalovich T, Hanson C. Food Addit. Contam. 2004; 21:555–563. [PubMed: 15204533]
42. He J, Shamsi SA. J. Sep. Sci. 2009; 32:1916–1926. [PubMed: 19479771]
43. Starkey JA, Mechref Y, Byun CK, Steinmetz R, Fuqua JS, Pescovitz OH, Novotny MV. Anal. Chem. 2002; 74:5998–6005. [PubMed: 12498195]
44. Zhang M, EI Rassi Z. Electrophoresis. 2001; 22:2593–2599. [PubMed: 11519964]
45. Schappler J, Guillarme D, Prat J, Veuthey J-L, Rudaz S. Electrophoresis. 2007; 28:3078–3087. [PubMed: 17724698]
46. Geiser L, Rudaz S, Veuthey J-L. Electrophoresis. 2003; 24:3049–3056. [PubMed: 12973809]
47. Takino M, Daishima S, Yamaguchi K. J. Chromatogr. A. 2000; 904:65–72. [PubMed: 11209902]
48. Andrea Raffaelli AS. Mass Spectrom. Rev. 2003; 22:318–331. [PubMed: 12949917]
49. Chauhan B, Gupta R. Process Biochem. 2004; 39:2115–2122.

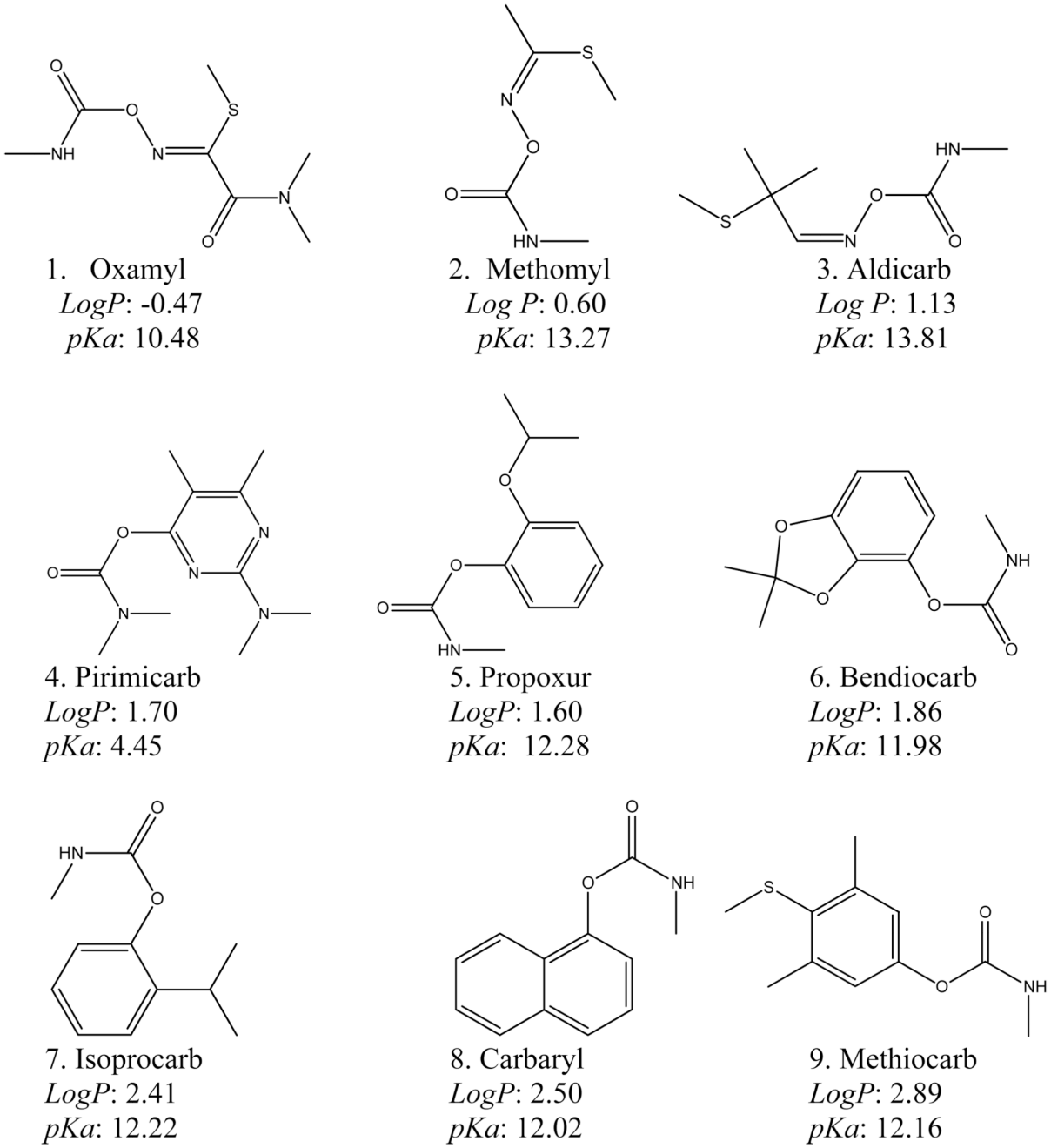

Figure 1.
Chemical structures of nine *N*-methylcarbamates (NCMs) studied in this work. Analytes are numbered according to their elution order. The *pKa* and log *P* were calculated using Advanced Chemistry Development (ACD/Labs) Software, Version 8.14 for Solaris.(1194–2006, ACD Labs).

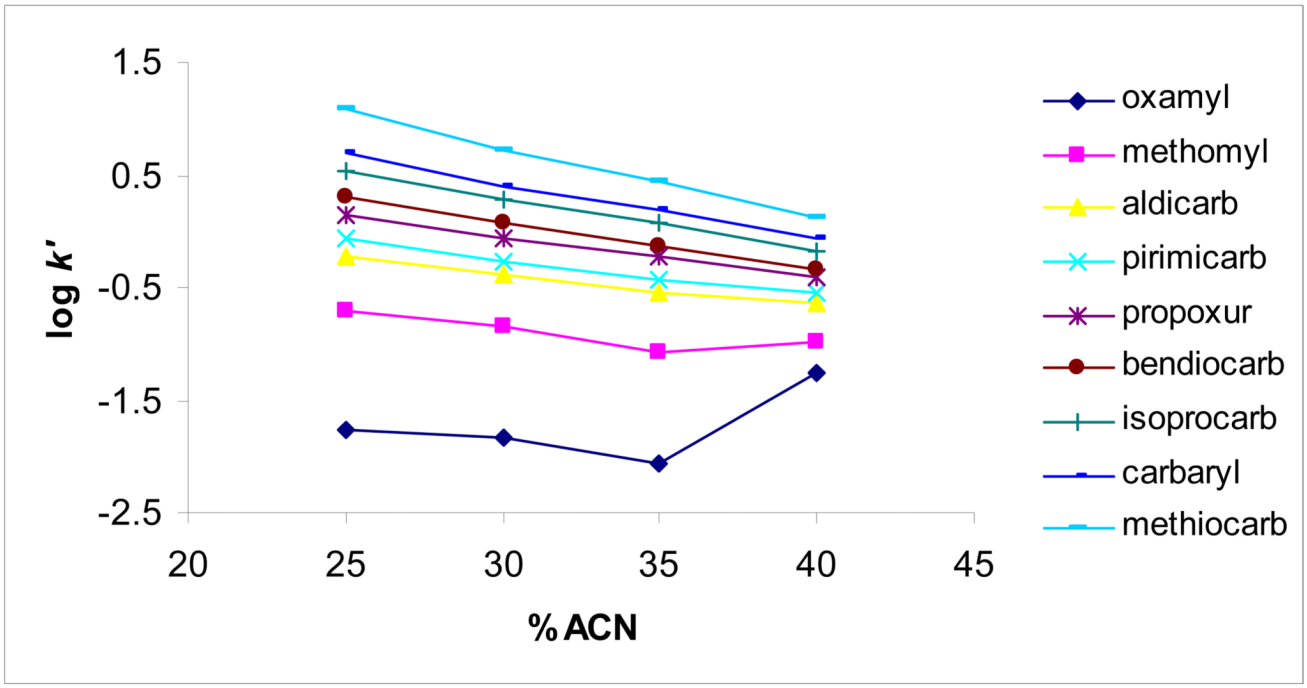

Figure 2.

The dependence of logarithmic capacity factor (*k´*) of NMCs on the concentration of ACN in the mobile phase. Experimental conditions: monolithic column, 40 cm (effective length) / 60 cm (total length) × 100μm ID; mobile phase, different concentration of ACN with 5 mM ammonium acetate, pH 6.5; applied voltage, 30 kV; electrokinetic injection, 5 kV for 3s; sample concentration, 100 ng/mL for each. APPI/MS parameters: sheath liquid composition, 50% methanol in water, 5mM ammonium, 2% acetone; sheath liquid flow rate, 5 μL/min; drying gas flow rate, 5L/min; nebulizer pressure, 5 psi; drying gas temperature, 200 °C; vaporizer temperature, 200 °C; capillary voltage, 2500 V; fragmentor voltage, 60 V.

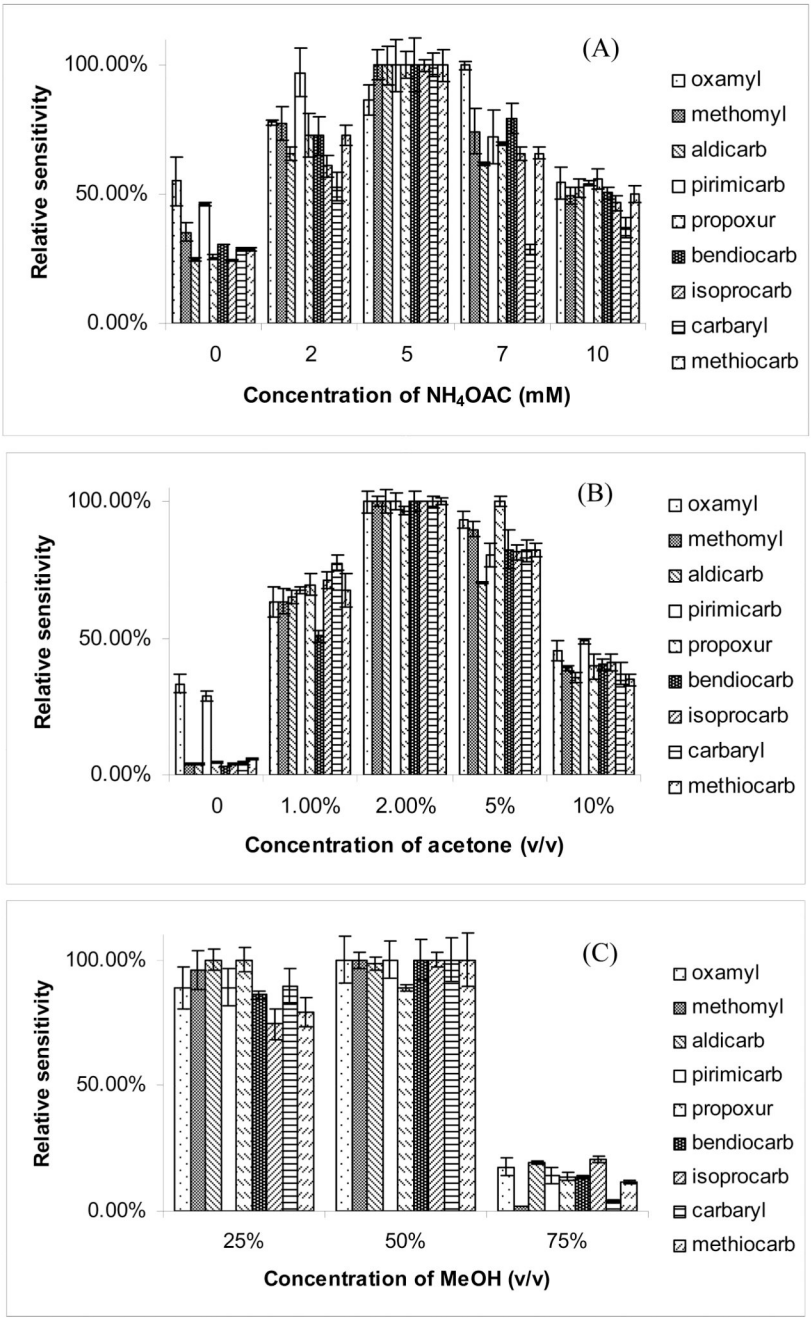

Figure 3.

The effect of (A) concentration of ammonium acetate, (B) concentration of acetone and (C) concentration of methanol in the sheath liquid on the sensitivity of APPI-MS. Experimental conditions: mobile phase, 35% ACN in 5 mM ammonium acetate, pH 6.5. Other conditions are the same as described in Fig. 2.

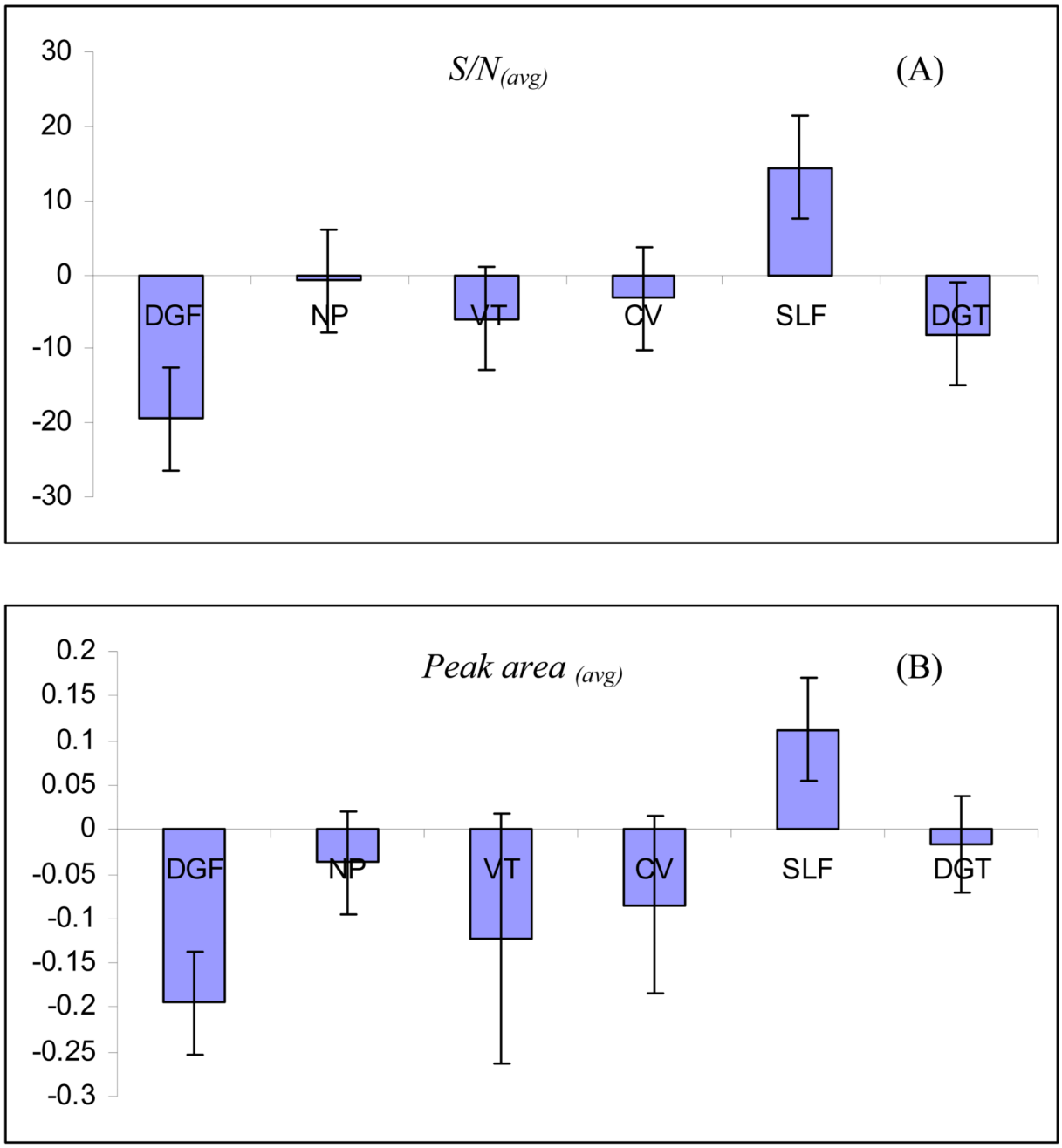

Figure 4.
The regression coefficient plots for (A) $S/N_{(avg)}$ and (B) *Peak area*$_{(avg)}$ obtained from FFD. Factors: drying gas flowrate (DGF); nebulizer pressure (NP); vaporation temperature (VT); capillary voltage (CV); sheath liquid flowrate (SLF) and drying gas temperature (DGT). Experimental conditions: monolithic capillary outlet position, −0.4 mm; sheath liquid composition, 50% methanol in water, 2% (v/v) acetone, 5 mM ammonium acetate. Other conditions are the same as mentioned in Fig. 3.

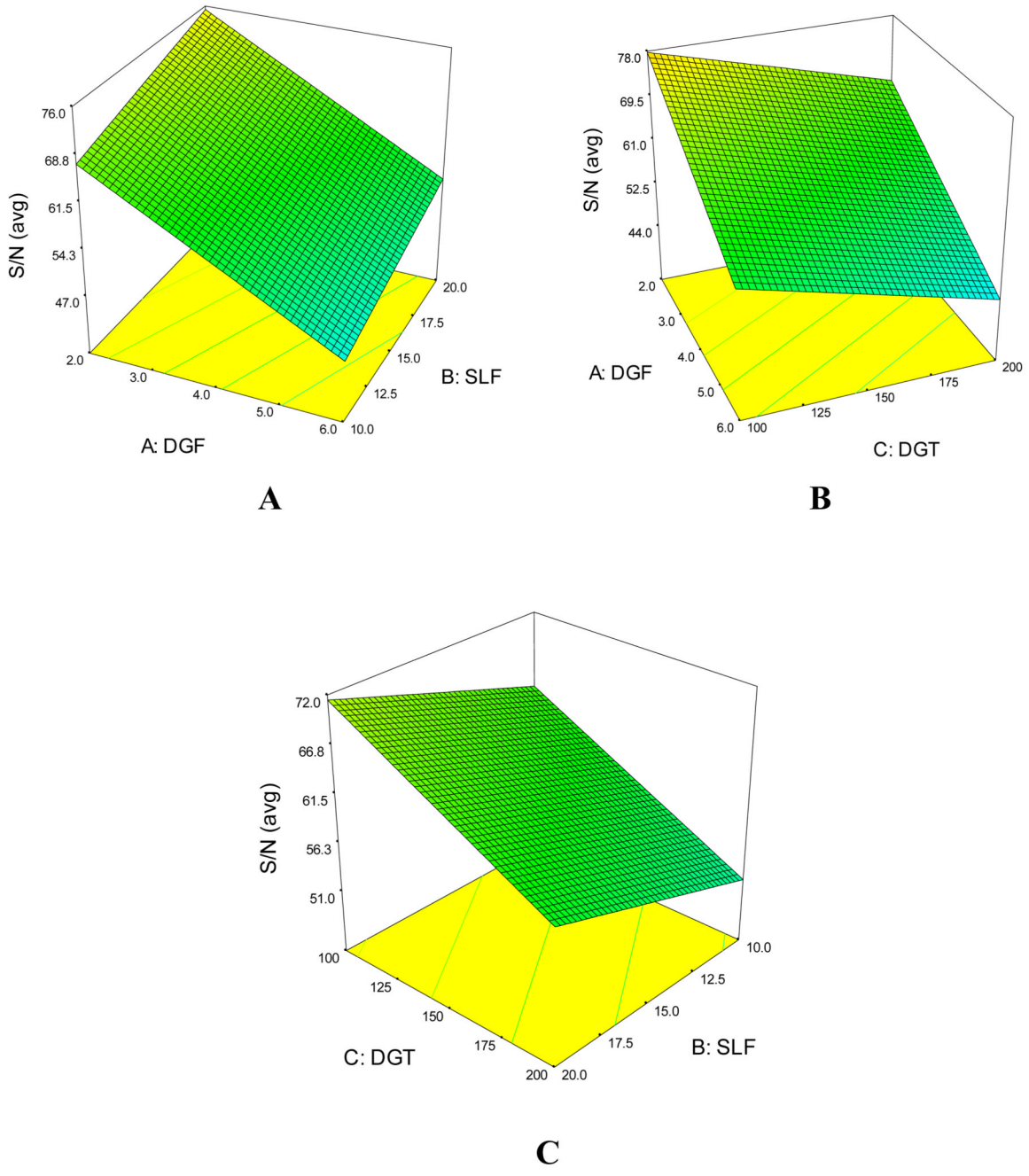

Figure 5.
The response surface plots obtained for (A) $S/N_{(avg)}$ and (B) *Peak area*$_{(avg)}$ of the nine NCMs as a function of significant factors: SLF and DGF.

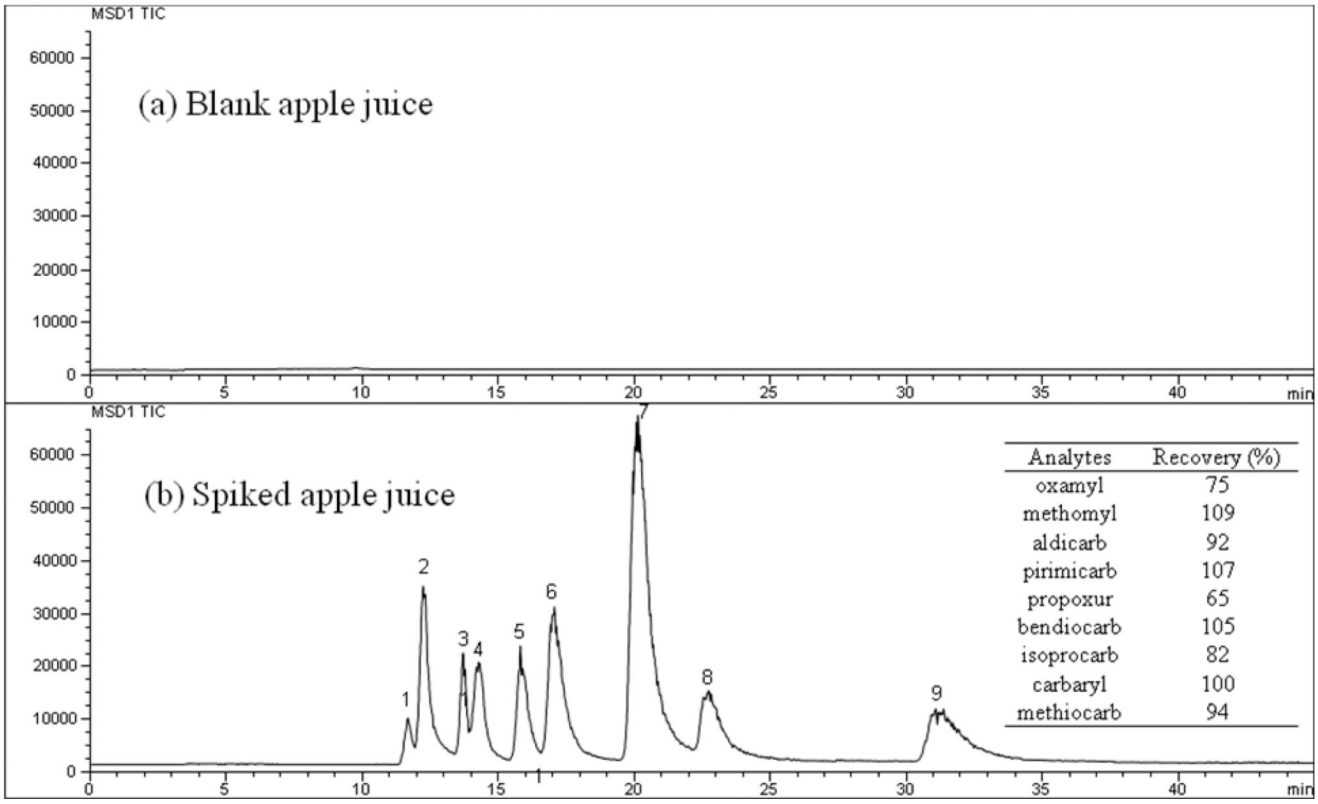

Figure 6.

The separation of blank apple juice (a) and NCMs pesticides spiked apple juice sample (b) on the AAUA-EDMA monolithic column in CEC-APPI-MS. Experimental conditions: monolithic column, 40 cm (effective length) /60 cm (total length) × 100μm ID; mobile phase, 35% ACN in 5 mM ammonium acetate, pH 6.5; applied voltage, 30 kV; electrokinetic injection, 5 kV for 3s; sample concentration, 100 ng/mL for each. APPI/MS parameters: sheath liquid composition, methanol-water (50:50, v/v), 5mM ammonium, 2% acetone; sheath liquid flow rate, 20 μL/min; drying gas flow rate, 2 L/min; nebulizer pressure, 5 psi; drying gas temperature, 200 °C; vaporizer temperature, 200 °C; capillary voltage, 2500 V; fragment voltage, 60 V; monolithic capillary outlet position, −0.4 mm. The inset table describes the recoveries of the nine NMCs.

Table 1

Selective ions used in the SIM mode.

Analytes	Molecular weight	Selective Ion (*m/z*)
Oxmayl	219	163[a]
Methomyl	162	163[b]
Aldicarb	190	116[c]
Pirimicarb	238	239[b]
Propoxur	209	210[b]
Bendiocarb	223	224[b]
Isoprocarb	193	194[b]
Carbaryl	201	202[b]
Methiocarb	225	226[b]

[a] $[M+NH_4\text{-}CH_3NHCOO]^+$.

[b] $[M+H]^+$.

[c] $[M+H\text{-}(CH_3NHCOOH)]^+$.

Table 2

Studied levels of parameters involved in fractional factorial design for screening the most important factors.

Variable factors	Level		
	Lower limit (−1)	Mean (0)	Upper limit (+1)
A: DGF (L/min)	2	6	10
B: NP (psi)	5	12.5	20
C: VT (°C)	200	250	300
D: CV (V)	1500	2500	3500
E: SLF (μL/min)	5	12.5	20
F: DGT (°C)	150	175	200

Table 3

Detail runs of fractional factorial design and the responses.

Run	A: DGF (L/min)	B: NP (psi)	C: VT (°C)	D:CV (V)	E:SLF (μL/min)	F: DGT (°C)	$S/N_{(avg)}$	$Peak\ area_{(avg)}$
1	2	5	300	3500	20	150	99.	6.2×10^5
2	2	5	200	1500	5	150	82	1.0×10^6
3	2	20	300	1500	5	150	41	2.8×10^5
4	10	20	300	1500	20	150	56	2.8×10^5
5	10	5	200	1500	20	150	48	4.5×10^5
6	2	20	200	3500	20	150	74	7.3×10^5
7	10	20	300	3500	20	200	34	1.9×10^5
8	10	5	300	1500	5	200	n.a.[a)]	n.a.[a)]
9	10	20	200	1500	5	200	18	3.1×10^5
10	10	5	200	3500	20	200	24	2.8×10^5
11	10	5	300	3500	5	150	n.a.[a)]	n.a.[a)]
12	2	20	300	3500	5	200	24	2.2×10^5
13	2	5	200	3500	5	200	56	4.9×10^5
14	2	5	300	1500	20	200	60	5.2×10^5
15	2	20	200	1500	20	200	83	9.9×10^5
16	10	20	200	3500	5	150	27	1.4×10^5
17	6	12.5	250	2500	12.5	175	80	2.4×10^5
18	6	12.5	250	2500	12.5	175	74	3.0×10^5
19	6	12.5	250	2500	12.5	175	68	2.9×10^5
20	6	12.5	250	2500	12.5	175	73	2.8×10^5
21	6	12.5	250	2500	12.5	175	72	2.7×10^5
22	6	12.5	250	2500	12.5	175	76	2.9×10^5

[a)] Data not available duo to ionization problem.

Electrophoresis. Author manuscript; available in PMC 2011 April 12.

Table 4

ANOVA table for models used in the screening of APPI parameters.

Responses	Source	Sum of squares	Degrees of freedom	Mean square	*F*-ratio	Prob>*F*	R^2	Adj-R^2	Pred-R^2	Ade-pre
$S/N_{(avg)}$	Model	1.1×10^{4}	6	1.9×10^{3}	11	0.0001				
	Residual	2.4×10^{3}	14	1.7×10^{2}						
	Lack of fit	2.1×10^{3}	9	2.3×10^{2}	4.0	0.0697				
	Pure error	2.9×10^{2}	5	57			0.82	0.75	0.48	13.8
	Corrected total	1.6×10^{4}	21							
$Peak\ area_{(avg)}$	Model	8.3×10^{-1}	6	1.4×10^{-1}	16	< 0.0001				
	Residual	1.0×10^{-1}	12	8.5×10^{-3}						
	Lack of fit	9.5×10^{-2}	7	1.4×10^{-2}	9.9	0.0114				
	Pure error	6.9×10^{-3}	5	1.4×10^{-3}			0.89	0.84	0.61	13.8
	Corrected total	1.0	19							

Table 5

Studied levels of parameters involved in central composite design for optimizing the most important factors.

Variable factors	Level		
	Lower limit (−1)	**Mean (0)**	**Upper limit (+1)**
A: DGF (L/min)	2	6	10
B: SLF (μL/min)	10	15	20
C: DGT (°C)	100	150	200

Table 6

Detail runs of CCD design and the responses.

Run	DGF	SLF	DGT	$S/N_{(avg)}$	$Peak\ area_{(avg)}$
1	4	15	150	77	4.7×10^5
2	6	20	100	65	$5..1\times10^5$
3	4	6.6	150	54	3.4×10^5
4	2	10	100	69	6.3×10^5
5	6	10	100	61	5.1×10^5
6	4	15	150	55	4.6×10^5
7	1	15	150	69	1.1×10^6
8	4	15	234	56	5.0×10^5
9	2	20	200	78	9.7×10^5
10	4	15	150	54	5.0×10^5
11	4	23	150	43	3.2×10^5
12	6	10	200	35	3.2×10^5
13	4	15	150	72	4.1×10^5
14	7	15	150	30	2.7×10^5
15	2	10	200	59	5.7×10^5
16	2	20	100	91	8.4×10^5
17	6	20	200	62	4.7×10^5
18	4	15	66	76	2.7×10^5
19	4	15	150	55	3.8×10^5
20	4	15	150	65	4.0×10^5

Electrophoresis. Author manuscript; available in PMC 2011 April 12.

Table 7

Regression coefficient of the coded factors and analysis of variance for the response surface models of $S/N_{(avg)}$ and $Peak\ area_{(avg)}$ for the optimization of APPI parameters.

Term	$S/N_{(avg)}$		$Peak\ area_{(avg)}$	
	Coefficient	**Prob>*F***	**Coefficient**	**Prob>*F***
Intercept	61.3	0.0062	5.14×10^5	0.0036
DGF	−10.2	0.0034	-1.84×10^5	0.0005
SLF	3.92	0.2068	526×10^2	0.2344
DGT	−6.27	0.0513	1.66×10^4	0.7019
R^2	0.73		0.86	
Adj-R^2	0.64		0.75	
Pred-R^2	0.52		0.64	
Ade-pre	8.3		8.8	

Table 8

Predicted values (obtained from Desirability Function) vs. experimental values (obtained from the actual experiment under optimized conditions) for $S/N_{(avg)}$ and $Peak\ area_{(avg)}$

	Predicted	Experimental	Difference
$S/N_{(avg)}$	70	78	+11%
$Peak\ area_{(avg)}$	1.05×10^6	9.66×10^5	−8.0%

Table 9

Calibration curves, regression coefficients (r^2), limit of detection (LOD, *S/N* =3) of the nine NMCs.

	Calibration curve	r^2	LOD (ng/mL)
oxamyl	y=92.08x−1566.2	0.9990	20
methomyl	y=586.15x−4427.1	0.9999	10
aldicarb	y=205.77x−9141.1	0.9989	30
pirimicarb	y=1000x+426.66	0.9999	3
propoxur	y=508.67x−4642.3	0.9998	12.5
bendiocarb	y=930.79x−573.33	0.9999	6
isoprocarb	y=2000x−5253.5	0.9999	4
carbaryl	y=736.62x−3003.4	0.9998	7
methiocarb	y=646.90x+3298.5	0.9999	12.5